

Hydrothermal synthesis of TiO₂ using TiCl₃ with Nutrients and gas sensing performance of TiO₂ thick films

Ganesh J. Mogal¹, G. E. Patil², F. I. Ezema³, V. B. Gaikwad⁴, Gotan H. Jain^{5*}

¹Materials Research Lab, K.T.H.M. College, Nasik 422013 India

^{2,5}Department of Physics, SNJBs K.K.H.A. Arts, S.M.G.L. Commerce and S. P. H. J. Science College, Chandwad 423101 India

³Director, BCUD, Savitribai Phule Pune University, Pune 411007

⁴Department of Physics & Astronomy, University of Nigeria, Nsukka, Enugu State, Nigeria

Abstract: In this work TiO₂ nanoparticles of hexagonal shape were prepared by using TiCl₃, the TiO₂ thick films were prepared by using screen printing technique. The films were characterized by scanning electron microscopy (SEM), UV visible technique, Transmission electron microscope (TEM) and Selected area diffractogram (SAED). The effect of change in nutrient such as water, NH₄ and seed of nano TiO₂ on the structural, morphological and gas sensing properties of the films were studied and discussed. Thick films of Hydrothermal synthesized TiO₂ using TiCl₃ and water is sensitive to LPG, When NH₄ is used as nutrient thick film were sensitive to H₂ gas and for TiO₂ nano seed it is sensitive to H₂S gas.

Keywords: Hydrothermal synthesis, TiO₂ nanoparticles, thick films, sensors.

Introduction

In past decades the titanium oxide is one of the most studied oxides for different application such as pigments, solar cell[1], biomaterials[2], photocatalysts[3], photovoltaics[4], electrochromic windows and displays[5-8] and sensing applications [9-12]. The different methods can be used to synthesis TiO₂ nanorods, nanotubes, nanoparticles and microspheres such as sol-gel method, Micelle and inverse micelle methods, sol method, solvothermal method, direct oxidation method, chemical vapor deposition, physical vapor deposition, electrode position, sonochemical, method, microwave method and hydrothermal method. There are several ways of preparing TiO₂ particles [13-16]. The hydrothermal method has many advantages like producing a highly homogeneous crystalline product, which can be obtained directly at relatively lower reaction temperature. Its most important feature is that decrease in agglomeration between particles, Phase homogeneity and controlled particle morphology. It also offers the uniform composition, purity of product, mono dispersed particles and control over the shape and size of the particles. In recent years, heterocontact between p and n-type semiconducting grains have been developed for detecting varies gases [17-20]. These semiconducting gas sensors possess a gas sensing mechanism different from single oxide semiconductors, and can detect small amount of toxic gases that exist in air. The most general gas sensing mechanism [12-17] of semiconductor gas sensors proposed is a simple resistivity change due to adsorption-desorption of gases. The p-n heterocontact concept was used in the present investigation [21-30]. There is an intrinsic difference in the behavior between the heterocontact type sensors and the sensors based on catalytic oxidation/reduction of gas molecules. The heterocontact type sensors work on the principle of barrier mechanism, which needs no adsorption and desorption of oxygen for the detection gas from air. In this work TiO₂ nanoparticles of hexagonal shape were prepared by using TiCl₃, the TiO₂ thick films were prepared by using screen printing technique and its gas sensing properties were investigated.

Experimental

A. TiO₂ powder preparation

To prepare TiO₂ powder, TiCl₃ were used as a source material. 20 ml of TiCl₃ was added in 2 ml dil HCl. NH₃ was drop wise added in solution. The solution was filtered and precipitate was dried for 3h.

B. Hydrothermal synthesis of TiO₂

The TiO₂ nano particles of rice grain shape were synthesized by a hydrothermal method. To prepare sample-A, 1 gm of TiO₂ powder was added in 160 ml water. The solution was stirred at room temperature for 20 min. The mixture was put into a Teflon-lined stainless autoclave which was heated at 180°C for 12h. For sample-B, 1 g of TiO₂ powder was added in 160 ml of liquid ammonia. Solutions were stirred at room temperature for 20 min. The mixture was put into a Teflon-

lined stainless autoclave which was heated at 180°C for 12h. For sample-C, mixing of 0.5 g of TiO₂ powder was 0.5 g TiO₂ seed (commercially prepared TiO₂ nano particles of size <25 nm) were added in 160 ml water. Solution was stirred at room temperature for 20 min. The mixture was put into a Teflon-lined stainless autoclave which was heated at 180°C for 12h. After heat treatment the sample A, B and C were naturally cooled to room temperature. The white precipitate was washed by de-ionized water and dried at 100°C for 2 h.

C. Preparation of TiO₂ thick film

The thixotropic paste was formulated by mixing the fine powder of Sample A (nano TiO₂) with the solution of ethyl cellulose (a temporary binder) in a mixture of organic solvent. The paste was screen printed on the glass substrate in the desired pattern. The film was fired at 550°C for 30 min. Silver contact was made for the electrical measurements. Similarly thick films using sample B and C were prepared.

D. Thickness measurements

The thickness of the films was observed in the range from 25 to 30 μm. The reproducibility in thickness of the films was possible by maintaining the proper rheology and thixotropy of the paste.

E. Details of gas sensing system

The sensing performance of the thick film sensors was examined using a 'static gas sensing system'. A heater was fixed on the base plate to heat the sample under test up to required operating temperatures. The Cr-Al thermocouple was used to sense the operating temperature of the sensor. The output of the thermocouple was connected to a digital temperature indicator. A gas inlet valve was fitted at one of the ports of the base plate. The required gas concentration inside the static system was achieved by injecting a known volume of a test gas using a gas-injecting syringe. A constant voltage was applied to the sensor, and the current was measured by a digital picoammeter. Air was allowed to pass into the glass chamber after every gas exposure cycle.

Result and Discussion

A. UV- visible spectra of synthesized TiO₂

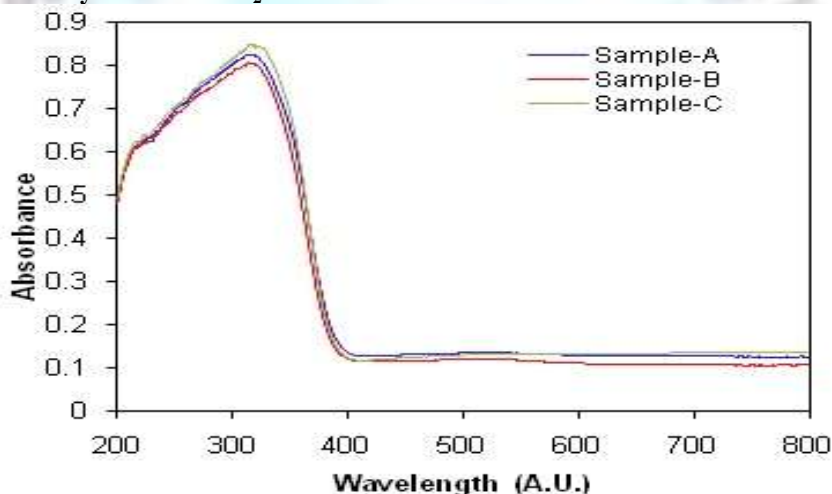


Fig. 1. U-V visible spectra of sample A, B and C.

Fig.1 shows the UV-visible spectra of hydrothermally synthesized TiO₂ powder. This spectra of TiO₂ is in the wavelength range of 200-800 A.U. The maximum absorbance is 0.83 for wavelength 332 A.U. and band gap is 3.73 eV, for sample A, B and C. The TiO₂ exists in three different crystal modifications, that is as anatase (tetragonal crystal structure with 3.2 eV energy gap [13]), rutile (tetragonal crystal structure with 3.2 eV energy gap), and brookite (orthorhombic with 2.96 eV energy gap). Among the three phases rutile is the most stable phase, which can be hydrothermally prepared.

B. X-Ray diffraction analysis

Fig.2 depicts an XRD pattern of TiO₂ powder (Sample A, B and C). X-ray diffraction analysis of this powder was carried out in the 20-80 deg. (2θ) range using Cu-Kα (with λ = 1.54 Å, 40 kV, 30 mA) radiation. The observed peaks matched well with the reported PDF 01-070-2556 [31] data confirming the polycrystalline nature. The higher peak intensities of an XRD pattern are due to the better crystalline nature. The percentage crystallinity is 92.2%, 93.1%, 93.4% and grain size were estimated to be 2.77 nm, 2.62 nm and 2.95 nm using Scherrer formula for Sample A, B and C respectively.

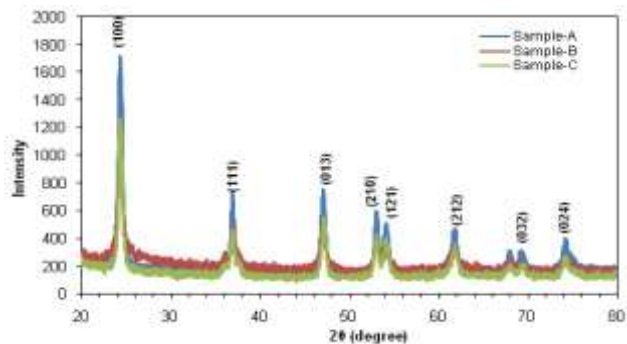


Fig. 2. X-Ray diffraction pattern of sample A, B and C.

C. Electrical conductivity of TiO₂ thick films

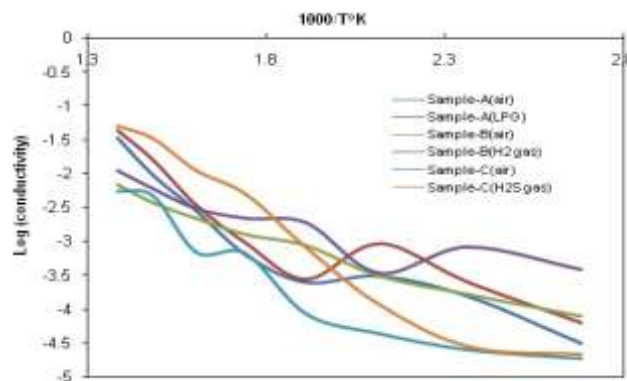


Fig.3. Variation of conductivity with temperature for TiO₂ thick films.

Fig.3 represents the variation of conductivity with temperature for thick films. It is clear from the graphs that the conductivity is varying approximately linearly with temperature. Conductivity of the films goes on increasing with an increase in temperature. Hence resistivity goes on decreasing with increase of temperature. Therefore, material exhibit negative temperature coefficient of resistance (NTC).

D. Microstructures analysis by SEM

The micro structural and chemical compositions of the films were analyzed using a scanning electron microscope (SEM, JEOL JED 6300) coupled with an energy dispersive spectrometer (EDS,JEOLJED2300LA). Fig. 4 (a, b and c) depicts a SEM image of TiO₂ thick film fired at 550° C(sample A,B and C). The films consist of voids and a wide range of particles distributed uniformly.

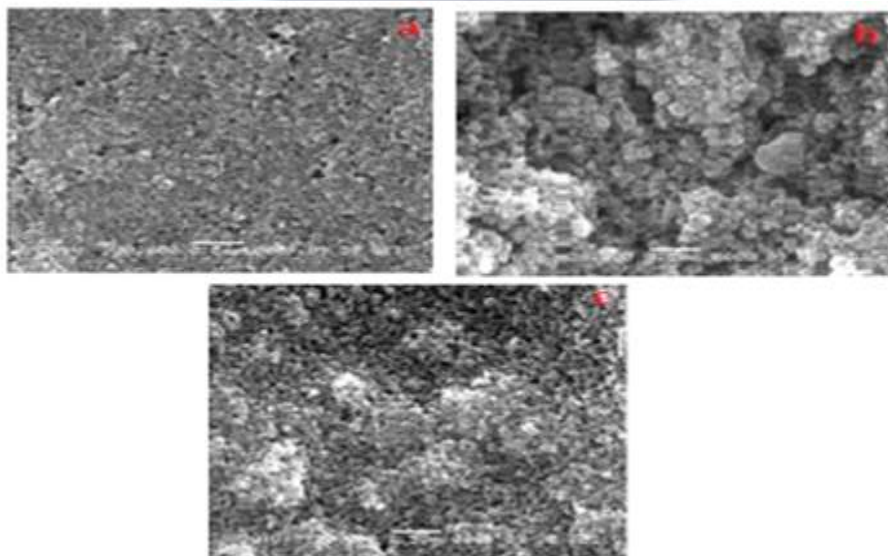


Fig. 4(a, b, c). SEM images of TiO₂ thick films.

E. TEM analysis

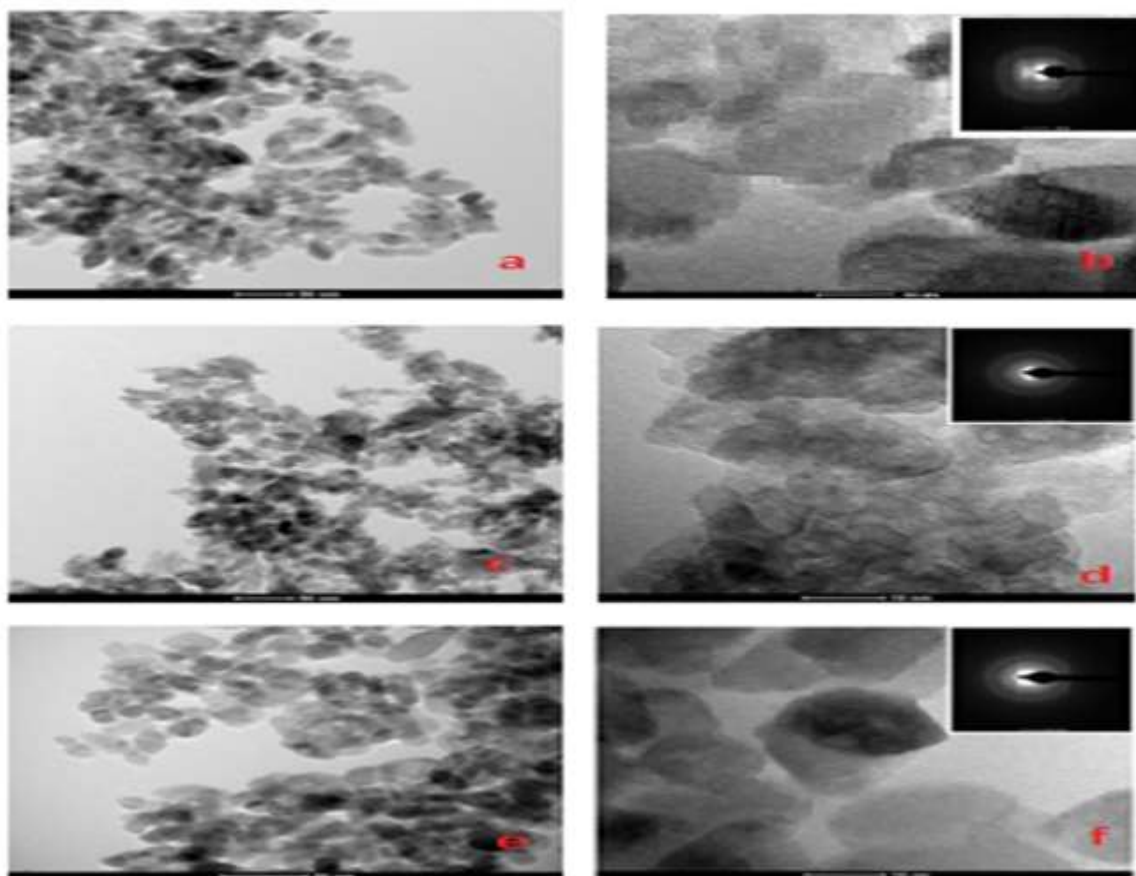


Fig. 5. TEM images of TiO₂ powder.

Fig.5 (a, c and e) shows TEM images of hydrothermally synthesized TiO₂ powder (sample-A, B and C) it shows rice grain like structure. Image (b, d and f) shows magnified TEM image and selected area diffraction pattern, it reveals that TiO₂ is predominantly single crystalline anatase with lattice spacing of 0.36nm. The atoms are arranged in definite manner and TiO₂ powder is well crystalline.

F. Sensitivity

Fig. 6 shows that for sample A the sensitivity of thick films was noted 20, which is maximum for LPG gas at operating temperature 200°C against all other tested gases. The thick film of sample-B shows sensitivity 14.11 for H₂ gas at operating temperature 150°C. The thick film of sample-C shows sensitivity 15 for H₂S gas at operating temperature 350°C.

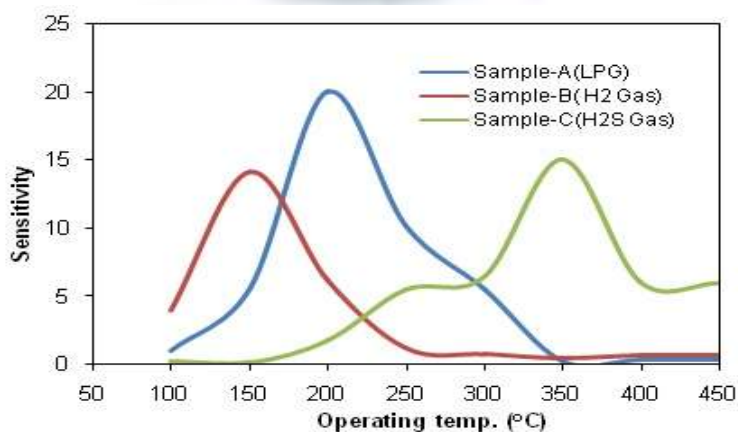


Fig. 6. Sensitivity of TiO₂ thick films.

G. Selectivity

Fig.7 shows that the TiO₂ thick film was selective to LPG gas (800 ppm) at 200°C against all other tested gases such as CO, CO₂, H₂, Cl₂, NH₃ and H₂S.

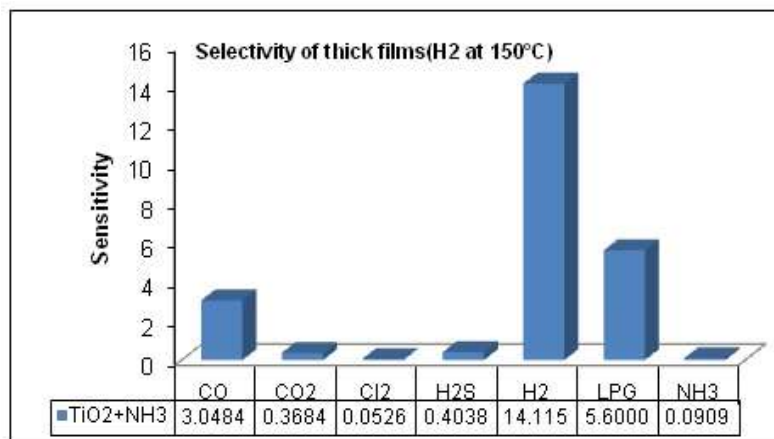


Fig. 7. Selectivity of TiO₂thick film (sample A).

Fig.8 shows that the TiO₂ thick film is selective to H₂ gas (800 ppm) at 150°C against all other tested gases such as CO, CO₂, LPG, Cl₂, NH₃ and H₂S.

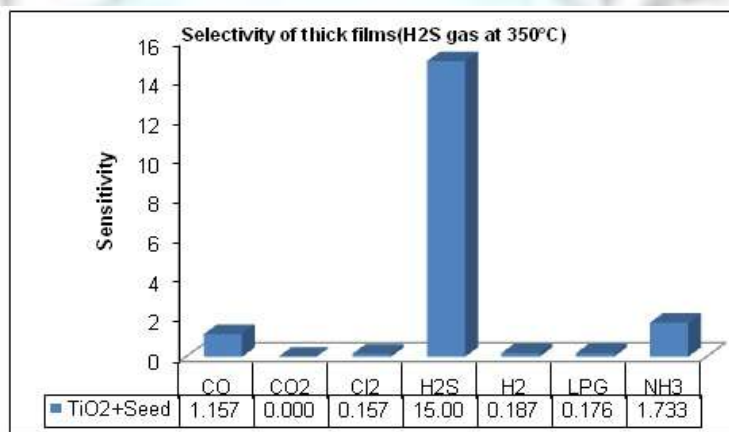


Fig. 8. Selectivity of TiO₂thick film (sample B).

Fig. 9 shows that the TiO₂ thick film was selective to H₂S gas (800 ppm) at 350°C against all other tested gases such as CO, CO₂, LPG, Cl₂, NH₃ and H₂.

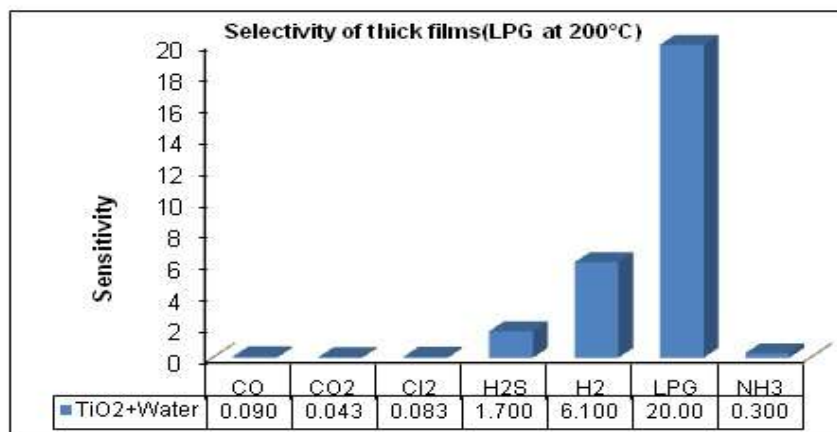


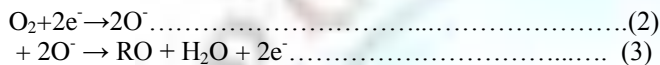
Fig. 9. Selectivity of TiO₂thick film (sample C).

H. Gas sensing mechanism

This is the most commonly accepted model for the operation of a semiconductor gas sensor, which presents a simplified model for a chain of ceramic grains. The physical model shows the grains with adsorbed oxygen on the surface, wherein the adsorbed oxygen has extracted electrons from the subsurface region of the grains leading to an insulating surface layer. In the bulk, however, the electrons are assumed to be plentiful. For conduction to occur, the electrons must pass from one grain to the other through this insulating layer. The Fig. 10 (b) shows the band model depicting this insulating layer in terms of the potential barrier. The extraction of electrons by the adsorbed oxygen from the surface leaves behind positively charged ions and consequently, an electric field develops between the positively charged ions and the negatively charged oxygen ions on the surface. For the conduction, the electrons in the conduction band must overcome the barrier associated with this electric field in order to move to the neighbouring grain. The barrier they must overcome is indicated as qV_s , where V_s increases as the concentration of O^- increases.

The density of electrons with sufficient energy to cross this barrier is n_s , given by the Boltzman equation:
 $n_s = N_d \exp(-qV_s/kT)$ (1)

With N_d the density of donors. The conductance through the film will be proportional to n_s . The more oxygen present on the surface, the higher the barrier and fewer electrons can make the transition and therefore the higher the resistance. The adsorbed oxygen is capable of causing a band bending up to 1eV at high coverages. The theoretically estimated coverage of the negatively charged species on the surface is limited to 10^{12} - 10^{13} cm^{-2} (Weisz limit). However, the coverage of this species is less than this limit under ambient conditions and hence, the potential barrier is less than 1eV. The overall chemical reactions assumed in this typical model are:



On exposure to a reducing gas (RH_2) the adsorbed oxygen reacts with the gas decreasing the potential barrier. Hence the electrons can overcome the potential barrier and the conductance increases.

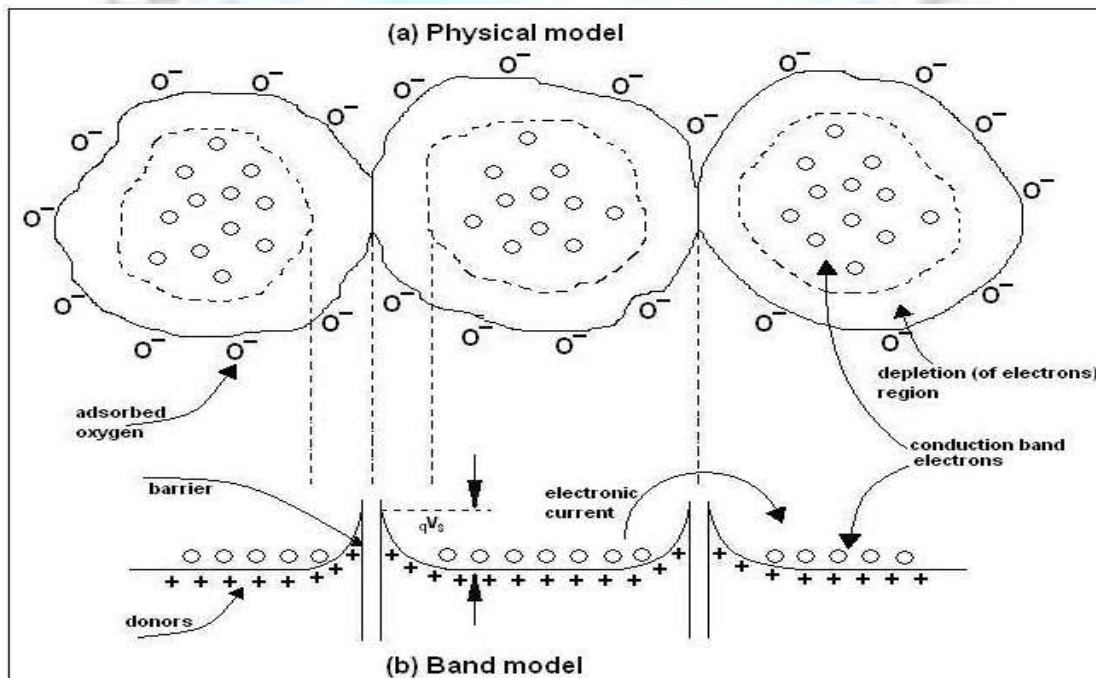


Fig.10. Model indicating the formation of potential barrier on oxygen adsorption. Physical model (a) and band model (b)

References

[1]. G. Ramakrishna and Hirendra N. Ghosh, Emission from the Charge Transfer State of Xanthene Dye-Sensitized TiO_2 Nanoparticles: A New Approach to Determining Back Electron Transfer Rate and Verifying the Marcus Inverted Regime, J. Phys. Chem. B 105 (2001) 7000–7008.
 [2]. J. Wu, S. Hayakawa, K. Tsuru, A. Osaka, In vitro bioactivity of anatase film obtained by direct deposition from aqueous titanium tetrafluoride solutions, Thin Solid Films 414 (2002) 275-280.

- [3]. M.Andersson,L.Osterlund,S.Ljungstrom,A.Palmqvist,Preparation of NanosizeAnatase and Rutile TiO₂ by Hydrothermal Treatment of Microemulsions and Their Activity for Photocatalytic Wet Oxidation of Phenol, *J. Phys. Chem. B* 106 (2002) 10674–10679.
- [4]. Michael Gratzel, Photoelectrochemical cells, *Nature* 414 (2001) 338-344.
- [5]. P. V. Kamat, Electrochromic and Photoelectro-chromic Aspects of Semiconductor Nanostructure- Molecular Assembly, in *The Electrochemistry of Nanostructures*, G. Hodes, Editor. (2001) Wiley-VCH: New York, 229-246.
- [6]. F. Pichot, S. Ferrere, R. J. Pitts, B. A. Gregg, Flexible Solid-State Photoelectrochromic Windows, *J.Electrochem.Soc.* 146 (1999) 4324-4326.
- [7]. Pen Hongmin,Bai Qingshun, Liang Yingchun and Chen Mingjun, Multiscale simulation of nanometric cutting of single crystalcopper effect of different cutting speeds, *Acta Metall. Sin. (Engl. Lett.)* 22 (2009) 440-446.
- [8]. A. E. Aliev, H. W. Shin, Nanostructured Materials for Electrochromic Devices, *Solid State Ion.*, 425 (2002) 154-155.
- [9]. G. K. Mor, K. Shankar, M. Paulose, O. K. Varghese and C. A. Grimes, Use of highly-ordered TiO₂ nanotubearrays in dye-sensitized solar cells, *NanoLett.*6 (2006) 5–8.
- [10]. G. K. Mor, K. Shankar, M. Paulose, O. K. Varghese and C. A. Grimes, Enhanced photocleavage of water usingtitania nanotube arrays, *NanoLett.*5 (2005) 1–5.
- [11]. M. Paulose, O. K. Varghese, G. K Mor, C. A. Grimes and K. G. Ong, Unprecedented ultra-high hydrogen gas sensitivity inundopedtitania nanotubes, *Nanotechnology* 17 (2006) 398–402.
- [12]. O. K. Varghese, D. Gong, M. Paulose, K. G. Ong, C. A. Grimes, Hydrogen sensing using titania nanotubes, *Sens. Actuators B* 93 (2003) 338-344.
- [13]. E. H. Poniatowski, R. Rodriguez-Talavera, C. Heredia, and O. Canocorona, R. Arroyo-Murillo, Crystallization of NanosizedTitania Particles Prepared by the Sol-gel Process, *J. Mater. Res.* 9 (1994) 2101–2108.
- [14]. W. Lee, Y. M. Gao, K. Dwight, A. Wold, Preparation and Characterization of Titanium (IV) Oxide Photocatalysts, *Mat. Res. Bull.* 27 (1992) 685–692.
- [15]. Q. Chen, Y. Qian, Z. Chen, G. Zhou, Y. Zhang, Preparation of TiO₂ Powders with Different Morphologies By An Oxidation Hydrothermal Combination Method, *Mater. Letts.* 22 (1995)77–80.
- [16]. Q. Chen, Y. Qian, Z. Chen, G. Zhou, Y. Zhang, Preparation of Ultrafine Powders of TiO₂ by Hydrothermal H₂O₂ Oxidation Starting From Metallic Ti, *J. Mater. Chem.* 3(1993) 203–205.
- [17]. E. Traversa, M. Miyayama, H. Yanagida, Gas sensitivity of ZnO/La₂CuO₄ heterocontacts, *Sens. Actuators B* 17 (1994) 257–261.
- [18]. J. Tamaki, T. Maekawa, N. Miura, N. Yamazoe, CuO–SnO₂ element for highly sensitive and selective detection of H₂S, *Sens. Actuators B* 9 (1992) 197–203.
- [19]. X. Zhou, Q. Cao, Y. Hu, J. Gao, Y. Xu, Sensing behavior and mechanismof La₂CuO₄–SnO₂ gas sensors, *Sens. Actuators B* 77 (2001) 443–446.
- [20]. X. Zhou, Q. Cao, H. Huang, P. Yang, Y. Hu, Study on sensing mechanism of CuO–SnO₂ gas sensors, *Mater. Sci. Eng. B* 99 (2003) 44–47.
- [21]. K. Kawakami, H.Yanagida, Effects ofwater vapor on the electrical conductivity of the interface of semiconductor ceramic–ceramic contact, *YogyoKyokaishiJpn.* 67 (1979) 112–115.
- [22]. Y. Nakamura, T. Tsurutani, M. Miyayama, K. Koamoto, H. Yanagida, The detection of carbon monoxide by the oxide-semiconductor heterocontacts, *J. Chem. Soc. Jpn.* (1987) 477–483.
- [23]. H. Ito, S. Fujisu, M. Miyayama, K. Koamoto, H. Yanagida, Alcohol sensor using p–n semiconductor contact, *J. Ceram. Soc. Jpn.* 100 (1992) 888–893.
- [24]. Y. Ushio, M. Miyayama, H. Yanagida, Fabrication of thin film CuO/ZnO hetero-junction and its humidity sensing properties, *Sens. Actuators B* 12(1993) 135–139.
- [25]. K. Hikita, M. Miyayama, H. Yanagida, New gas sensing method for detecting carbon monoxide by use of the complex impedance of CuO/ZnOheteroconductor under a dc bias voltage, *J. Am. Ceram. Soc.* 77 (1994)1761–1764.
- [26]. H. Hirota, M. Mayayama, Y. Nakamura, H.Yanagida, Quantitative analysisof ethanol in water solution by a heterocontact type sensor of CuO/ZnO, *Chem. Lett. Jpn.* (1994) 1793–1796.
- [27]. D.J. Yoo, J. Tamaki, S.J. Park, N. Miura, N. Yamazoe, Copper oxide loaded tin dioxide thin film for detection of dilute hydrogen sulphide, *Jpn. J. Appl.Phys.* 34 (1995) 455–457.
- [28]. S.J. Jung, H. Yanagida, The characterization for a CuO/ZnOheterocontact type gas sensor having selectivity for CO gas, *Sens. Actuators B* 37 (1996) 55–60.
- [29]. R.B. Vasilier, M.N. Romyantseva, M.N. Yakovlev, A.M. Gaskov, CuO/SnO₂ thin film heterostructures as chemical sensors to H₂S, *Sens. Actuators B* 50 (1998) 186–193.
- [30]. M.S. Wagh, L.A. Patil, D.P. Amalnerkar, Surface cupricated SnO₂–ZnO thick films as a H₂S gas sensor, *Mater. Chem. Phys.* 84 (2004) 228–233.
- [31]. D. J. Lacks, R. G. Gordon, Crystal structure calculation with distorted ions, *Phys.Rev. B* 48(1993)2889-2908.